The American Journal of Pathology, Vol. 175, No. 5, November 2009

DOI: 10.2353/ajpath.2009.090463

Cell Injury, Repair, Aging and Apoptosis

Enhancement of Autophagic Flux after Neonatal Cerebral Hypoxia-Ischemia and Its Region-Specific Relationship to Apoptotic Mechanisms

Vanessa Ginet,*† Julien Puyal,† Peter G.H. Clarke,† and Anita C. Truttmann*

From the Division of Neonatology, Department of Pediatrics and Pediatric Surgery, University Hospital Center, Switzerland; and the Department of Cellular Biology and Morphology,† University of Lausanne, Lausanne, Switzerland*

The multiplicity of cell death mechanisms induced by neonatal hypoxia-ischemia makes neuroprotective treatment against neonatal asphyxia more difficult to achieve. Whereas the roles of apoptosis and necrosis in such conditions have been studied intensively, the implication of autophagic cell death has only recently been considered. Here, we used the most clinically relevant rodent model of perinatal asphyxia to investigate the involvement of autophagy in hypoxic-ischemic brain injury. Seven-day-old rats underwent permanent ligation of the right common carotid artery, followed by 2 hours of hypoxia. This condition not only increased autophagosomal abundance (increase in microtubule-associated protein 1 light chain 3-11 level and punctuate labeling) but also lysosomal activities (cathepsin D, acid phosphatase, and β-N-acetylhexosaminidase) in cortical and hippocampal CA3-damaged neurons at 6 and 24 hours, demonstrating an increase in the autophagic flux. In the cortex, this enhanced autophagy may be related to apoptosis since some neurons presenting a high level of autophagy also expressed apoptotic features, including cleaved caspase-3. On the other hand, enhanced autophagy in CA3 was associated with a more purely autophagic cell death phenotype. In striking contrast to CA3 neurons, those in CA1 presented only a minimal increase in autophagy but strong apoptotic characteristics. These results suggest a role of enhanced autophagy in delayed neuronal death after severe hypoxia-ischemia that is differentially linked to apoptosis according to the cerebral region. ***(Am J Pathol 2009, 175:1962–1974; DOI: 10.2353/ajpath.2009.090463)***

Despite increasing research on animal models of perinatal asphyxia and important advances toward understanding its pathophysiology, up to now, no pharmacological treatment is recognized and perinatal asphyxia remains a major cause of mortality or serious long-term motor and cognitive disabilities including cerebral palsy, seizure disorders and mental retardation.[1–3] One of the main difficulties for developing a neuroprotective pharmacotherapy is the existence of multiple cellular death mechanisms, occurring in different cells or even in the same cell,[4,5] which may all need to be inhibited. In fact, the widely accepted apoptosis-necrosis dichotomy is being replaced by a more complex view involving a third type of cell death, named autophagic cell death (type II), characterized by the presence of intense autophagy.[6,7]

Autophagy is an essential pathway for the degradation and recycling of intracellular macromolecules. The most important autophagic mechanism, macroautophagy, consists in the sequestration of long-lived proteins and damaged organelles in multimembrane vesicles, named autophagosomes, which then fuse with lysosomes to degrade their contents.[8] Whereas basal macroautophagy (called hereafter autophagy) plays a central physiological function in maintaining cellular homeostasis, induced autophagy may have both survival and deleterious roles.[9] In neurons, autophagy has been demonstrated to be induced during development, starvation, neurodegeneration,[10] and also after different excitotoxic stimuli.[11–14] More recently, an involvement of enhanced

Supported by Swiss National Science Foundation (3100A0-105824; to A.C.T. and 3100A0-113925; to P.G.H.C. and J.P.), Fondation Motrice (2007-08; to P.G.H.C. and 2008-09; to ACT), and the Eagle Foundation (to A.C.T. and P.G.H.C.).

V.G. and J.P. contributed equally to the work.

Accepted for publication July 30, 2009.

Supplemental material for this article can be found on *http://ajp.amjpathol.org*.

Address reprint requests to Dr. Anita C. Truttmann, M.D., Division of Neonatology, Department of Pediatrics and Pediatric Surgery, University Hospital Center and University of Lausanne, 1011 Lausanne, Switzerland. E-mail: anita.truttmann@chuv.ch.

autophagy in neuronal death following cerebral ischemia has been proposed.[15–18]

The Rice-Vannucci hypoxia-ischemia (HI) model is accepted to be the most clinically relevant rodent model of perinatal asphyxia.[19] Recently, an increase in autophagosome formation was described in this model performed in mice[15,18] suggesting an enhancement of autophagy after neonatal cerebral HI. However, it is not clear whether this increase was due to a defect in lysosomal function causing an accumulation of autophagosomes, as described in neurodegenerative disorders such as Alzheimer's disease,[20] or to an increase in autophagic flux, ie, the whole process of autophagy.

In the present study, we have investigated the involvement of autophagy after severe cerebral HI in neonatal rats and have shown not only an increase in the abundance of autophagosomes but also an enhancement of lysosomal activity. Taken together, these two observations imply an increase in autophagic flux. Moreover our results showed important differences in the relationship between enhanced autophagy and apoptosis in the cortex and the hippocampus and highlight striking differences in the cell death mechanisms induced in CA3 and CA1.

Materials and Methods

Animal Model

All experiments were performed in accordance with the Swiss Laws for the protection of animals and were approved by the Vaud Cantonal Veterinary Office.

HI was induced in 7-day-old male rats (16 to 19 g; Sprague Dawley, Janvier, France) according to the Rice-Vannucci modification[19] of the Levine procedure.[21] The rat pups were anesthetized with 3% isoflurane. The right common carotid artery was isolated, double-ligated (Silkam, 5/0; B/BRAUN Aesculap, Center Valley, PA) and cut. After 2 hours of recovery with the dam, pups were placed in a humidified chamber at 35.5°C with 8% oxygen. To obtain a reproducible lesion volume we selected a hypoxic period of 2 hours, which produced substantial damage affecting most of the ipsilateral hemisphere. After hypoxia, pups were returned to the dam until sacrifice. Sham animals underwent the described anesthetic and surgical procedure but without section of the common carotid artery.

Immunohistochemistry

Pups were deeply anesthetized with an i.p. injection of 150 mg/kg sodium-pentobarbital and then perfused transcardially with 4% paraformaldehyde in 0.1 mol/L PBS (pH 7.4) at 6 hours or 24 hours after HI.

Immunohistochemistry was performed on 18-μm cryostat sections. For immunoperoxidase labeling, the mounted sections were immersed for 20 minutes in 0.3% H_2O_2 in methanol to quench endogenous peroxidases and then rinsed in PBS and preincubated for 45 minutes in 15% serum and 0.3% Triton X-100 in PBS. They were then incubated overnight with the primary antibody in 1.5% serum and 0.1% Triton in PBS, washed in PBS and incubated with the biotinylated secondary antibody (Jackson ImmunoResearch Laboratories, West Grove, PA) for 2 hours at room temperature. After 3 PBS washes they were incubated in avidin–biotin–peroxidase complex (ABC Reagent; Vector Laboratories, Burlingame, CA) for 2 hours at room temperature and then developed by incubation with diaminobenzidene (Roche, Mannheim, Germany) substrate solution until the desired intensity of staining was obtained. The sections were finally dehydrated in graded alcohols and mounted in Eukitt.

For immunofluorescence labeling, the sections were preincubated for 45 minutes in 15% serum and 0.3% Triton X-100 in PBS and then incubated overnight at 4°C with the primary antibody in 1.5% serum and 0.1% Triton in PBS, washed in PBS, and incubated for 2 hours in fluorochrome-coupled secondary antibody (Alexa Fluor 488 or Alexa Fluor 647 from Molecular Probes, Eugene, OR) at room temperature. The sections were then rinsed in PBS and mounted with FluorSave (Calbiochem, San Diego, CA) with or without the nuclear stain 4′,6′-diamidino-2-phenylindole (Vector Laboratories). A LSM 510 Meta confocal microscope (Carl Zeiss, Thornwood, NY) was used for confocal laser microscopy. Confocal images were displayed as individual optical sections. For double-labeling, immunoreactive signals were sequentially visualized in the same section with two distinct filters, with acquisition performed in separated mode. Images were processed with LSM 510 software and mounted using Adobe Photoshop.

The antibodies used were as follows: anti-microtubule-associated protein 2 rabbit (AB5622; 1/200), anti-NeuN (MAB377; 1/200) and anti-cathepsin D (06-467; 1/200) from Millipore (Temecula, CA), anti-LAMP1 (428017; 1/200) from Calbiochem (La Jolla, CA), anti-cathepsin D (sc-6486; 1/200) from Santa Cruz Biotechnology (Santa Cruz, CA), and anti-cleaved caspase-3 (9661; 1/200) from Cell Signaling Technologies (Danvers, MA). The anti-cleaved caspase-3 antibody was verified by immunoblotting to recognize only the active caspase-3 form (data not shown). Anti microtubule-associated protein 1 light chain 3 (LC3) was a gift from Prof. Y. Uchiyama (Tokyo, Japan; 1/2000).

Terminal Deoxynucleotidyl Transferase-Mediated dUTP Nick-End Labeling

Terminal deoxynucleotidyl transferase-mediated dUTP nick-end labeling (TUNEL) staining was obtained with an *in situ* cell death detection kit (Roche Applied Science, Nonnenwald, Germany), according to the manufacturer's instructions. The mounted sections were incubated for 2 minutes in a freshly prepared aqueous solution of 0.1% Triton X-100 and 0.1% sodium citrate, covered with 50 μl of TUNEL mixture for 1 hour at 37°C, rinsed in PBS, and mounted with FluorSave. For peroxidase revelation of TUNEL, sections were incubated for 2 hours at room temperature with an anti-FITC antibody conjugated with biotin (Sigma-Aldrich, St. Louis, MO).

Immunoblotting

Pups were decapitated at 30 minutes, 4 hours, 6 hours, or 24 hours after HI, and the brains were removed in 0.1mol/L PBS containing 1 mmol/L $MgCl_2$ on ice. The different cerebral regions (cortex, hippocampus, thalamus, and striatum) were dissected out and collected in lysis buffer containing 20 mmol/L HEPES (pH 7.4), 10 mmol/L NaCl, 3 mmol/L $MgCl_2$, 2.5 mmol/L EGTA, 0.1 mmol/L DTT, 50 mmol/L NaF, 1 mmol/L Na_3VO_4NaF, 1% Triton X-100, and a protease inhibitor mixture (Roche). Tissues were sonicated, and protein concentration was determined using a Bradford assay. Proteins (20 to 40 μg) were separated on SDS-PAGE (10 or 15% polyacrilamide) and transferred to polyvinylidene difluoride membranes. Then the membranes were blocked in 5% nonfat milk in TBS-T (200 mmol/L Tris and 1.5mol/L NaCl with 0.1% Tween 20) and were incubated with primary antibody diluted in the blocking solution overnight at 4°C. The membranes were washed and incubated with secondary horseradish peroxidase-coupled antibodies (Pierce Biotechnology, Rockford, IL) in TBS-T 1% milk for 1 hour at room temperature. After the final washes, the proteins were detected by enhanced chemiluminescence. The bands were quantified using ImageQuant TL software (Amersham Biosciences) and values were normalized with respect to tubulin. The values were then expressed as a percentage relative to the sham level of OD. The antibodies used were as follows: anti-LC3 (PD012) from MBL (Naka-Ku Nagoya, Japan; 1/1000), anti-cleaved caspase-3 (1/1000) from Cell Signaling Technologies, anti-fodrin (FG6090; 1/3000) from BIOMOL (Plymouth Meeting, PA), and anti-tubulin (SC-8035; 1/5000) from Santa Cruz Biotechnology.

Histochemistry for Lysosomal Enzymes

Rat pups were anesthetized and perfused intracardially with 2% glutaraldehyde and 1% paraformaldehyde in cacodylate buffer (0.1 mol/L (pH 7.4)). Brains were removed and postfixed in the same fixative solution overnight at 4°C, then washed three times in 0.1 mol/L cacodylate buffer (pH 7.3). Coronal vibratome sections (30 to 50 μm) were cut and stained as described below.

Acid Phosphatase Histochemistry

The activity of acid phosphatase (AP) was studied by histochemistry using sodium β-glycerophosphate with lead nitrate as substrate (modification of Gömöri's sodium β-glycerophosphatase method).[22] Briefly, after several washes in distilled water, sections were incubated for 2 hours at 37°C in filtered 0.01 mol/L sodium β-glycerophosphate and 8 μmol/L lead nitrate in sodium acetate buffer (50 mmol/L (pH 5)). After incubation, sections were rinsed in distilled water and immersed in ammonium sulfide (0.5%) for 30 seconds, rinsed again, dehydrated in graded alcohols, and mounted in Eukitt. The enzyme cleaves the sodium β-glycerophosphate in an acidic environment to produce free phosphate ions, which combine with the lead ions to produce insoluble lead phosphate. Treatment with ammonium sulfide gives lead sulfide, which forms black precipitates. Controls were performed using the AP inhibitor NaF (10 mmol/L).

β-N-Acetylhexosaminidase Histochemistry

The procedure of Katayama et al[23] was used. Briefly, sections were washed in distilled water and then incubated for 1 hour at 37°C in Fast red violet salt solution (0.63mol/L ethylene glycol monomethyl ether, 1% polyvinyl pyrrolidone, 0.1 mol/L citric acid-citrate buffer (pH 4.4), 1.6 mol/L sodium chloride, 2.7 mmol/L 5-chloro-4-benzamido-2-methylbenzene-diazonium chloride (Fast red violet LB salt) (Sigma-Aldrich) using 0.5mmol/L naphthol-AS-BI-*N*-acetyl-β-D-glucosaminide (Sigma-Aldrich) as the substrate. The sections were then rinsed in distilled water and fixed for 10 minutes in 10% formaldehyde, then rinsed twice with distilled water, dehydrated in graded alcohols and mounted in Eukitt medium. To verify the staining specificity, controls with omission of the substrate or at basic pH (pH 10) were done in parallel.

Enzyme Assay for Acid Phosphatase

Brains were removed in 0.1mol/L PBS containing 1 mmol/L $MgCl_2$ on ice at 6 or 24 hours after HI. The cortex and the hippocampus were dissected out and collected in the same lysis buffer as for immunoblotting but without NaF and Na_3VO_4. Tissues were sonicated, and protein concentration was determined using a Bradford assay. Ten micrograms of proteins diluted in sodium acetate buffer (0.1 mol/L (pH 5.5)) and 20 mmol/L *p*-nitrophenyl phosphate was incubated 2 hours at 37°C in a final volume of 400 μl. The reaction was stopped by the addition of 50 μl of 2 mol/L NaOH, and absorbance was measured at 405 nm.

Electron Microscopy

Rat pups were perfused intracardially with 2.5% glutaraldehyde and 2% paraformaldehyde in cacodylate buffer (0.1 mol/L (pH 7.4)). The brains were postfixed overnight at 4°C in the same fixative. Coronal vibratome sections (50 to 200 μm) were cut, rinsed in cacodylate buffer, postfixed in osmium tetroxide (1% in cacodylate buffer) for 30 minutes, and contrasted in uranyl acetate (1% in ethanol 70%) for 5 minutes. The sections were then dehydrated in graded alcohols and embedded in Durcarpan ACM resin (Fluka, Neu-Ulm, Germany) between silicon-coated glass slides. Ultrathin sections (at silver to gray interference) were cut with a diamond knife (Diatome), mounted on formvar-coated single-slot grids, contrasted with uranyl acetate and alkaline lead citrate, and visualized using a Philips CM10 transmission electron microscope.

Statistics

Data were expressed as mean ± SEM. Values were verified to be normally distributed and analyzed statisti-

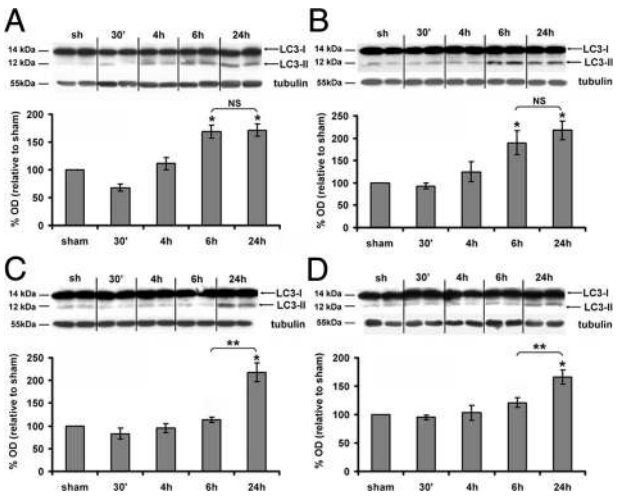

Figure 1. Effect of hypoxia-ischemia on LC3-II expression. **A–D:** Representative immunoblots of LC3 (**upper panel**) and the corresponding quantifications of the LC3-II form (**lower panel**) relatively to the sham level show that hypoxia-ischemia increases significantly the LC3-II expression levels from 6 hours in the cortex (**A**) and hippocampus (**B**), from 24 hours in the thalamus (**C**) and striatum (**D**). Data represent mean ± SEM. Comparisons by *t*-test: $^{*}P < 0.01$ with sham, $^{**}P < 0.01$ between 6 and 24 hours. NS, not significant ($n \geq 4$).

cally by one-way analysis of variance, followed by Student's *t*-test (one-tailed, two samples, and unequal variance). Probability values of $P < 0.05$ were considered to be significant. The Bonferroni correction was used to adjust for multiple comparisons.

Results

Increase in Autophagosomes after Neonatal Cerebral HI

To study the presence of autophagosomes following cerebral HI, we first performed Western blots against LC3. LC3 is a crucial Atg (autophagic-related gene) protein involved in autophagosome formation. When autophagy is induced, LC3-I (cytosolic) is successively modified and linked to a phosphatidylethanolamine leading to the LC3-II form, which is recruited to the membrane of the autophagosome. In the present study, LC3-II expression, which is directly related to the number of autophagosomes, was analyzed in four different affected cerebral regions (cortex, hippocampus, thalamus, and striatum) at different time points after HI. As shown in Figure 1, HI induced a significant increase in LC3-II levels 24 hours after HI in each region in comparison with a sham animal. Moreover, regional differences in the timing of LC3-II increases were observed. LC3-II levels reached their maximum values as early as 6 hours post-HI in the cortex (6 hours: 167 ± 12%; 24 hours: 171 ± 11%; Figure 1A) and hippocampus (6 hours: 190 ± 27%; 24 hours: 218 ± 20%; Figure 1B) but only at 24 hours post-HI in the thalamus (6 hours: 120 ± 8%; 24 hours: 166 ± 13%; Figure 1C) and striatum (6 hours: 113 ± 6%; 24 hours: 217 ± 21%; Figure 1D). Because LC3-II increase occurred more rapidly in the cortex and in the hippocampus, we focused further our investigations on these two regions.

Immunohistochemistry against LC3 showed that in sham animals LC3 labeling was diffuse, faint and homogenously distributed in the cytosol of cortical and hippocampal cells (Figure 2). After HI, some cortical cells, mainly located at the border of the lesion, displayed strong labeling as compared with sham cortex (Figure 2, A and D). High magnification views revealed the presence of numerous LC3-positive dots in the cytosol of these cells. In the hippocampus, regional differences in LC3 immunolabeling were observed. CA1 displayed only a few cells labeled after HI, whereas LC3 labeling was strongly increased in CA3 cells (Figure 2, B and E, for CA3, and Figure 2C for CA1). Double immunolabeling against LC3 and the neuronal marker Neuronal Nuclei (NeuN) showed that the increase in LC3 punctate labeling occurred in neurons as shown for the cortex and CA3 (Figure 2, D and E). The number of punctate LC3-positive neurons strongly decreased at 48 and 72 hours (data not shown). Double labeling between LC3 and several glial markers (such as glial fibrillary acidic protein and S100β) showed no co-localization (data not shown).

Increase in Lysosomes/Autolysosomes after Neonatal Cerebral HI

Immunohistochemistry revealed a strong increase in lysosomal-associated membrane protein 1 (LAMP1) (Figure 3) and the lysosomal protease cathepsin D (Figure 4) from 6 hours after HI in the cortex and hippocampus. At high magnification, both the size and the number of LAMP1- and cathepsin D-positive dots in the cytosol were seen to be increased. In the hippocampus, strong increases in LAMP1 (Figure 3, B and C) and cathepsin D (Figure 4, B and C) were restricted to CA3. Double immunolabeling showed that the strong expression of LAMP1 (Figure 3, D and E) and cathepsin D (Figure 4, D and E) occurred mainly in cells expressing, respectively, microtubule-associated protein 2 and NeuN, demonstrating that these increases in lysosomal markers occurred in neurons.

Lysosomal/Autolysosomal Activities after Neonatal Cerebral HI

To investigate whether these increases in lysosomal staining were related to an increase in lysosomal activities following HI, we performed histochemistry and/or enzymatic assays against two lysosomal enzymes, AP and β-N-acetylhexosaminidase (AcHex) (Figure 5).

In sham cortex and hippocampus, AP histochemistry showed cells with only a few small AP-positive dots (presumably lysosomes), indicating a low basal AP activity. From 6 hours after HI, cortical (Figure 5A) and CA3 neurons (Figure 5B), but not CA1 neurons (Figure 5C), displayed an increase in the number and size of AP-positive dots, indicating presumably the appearance of autolysosomes. This enhanced AP activity was confirmed by enzyme assay on protein extracts of the whole cortex

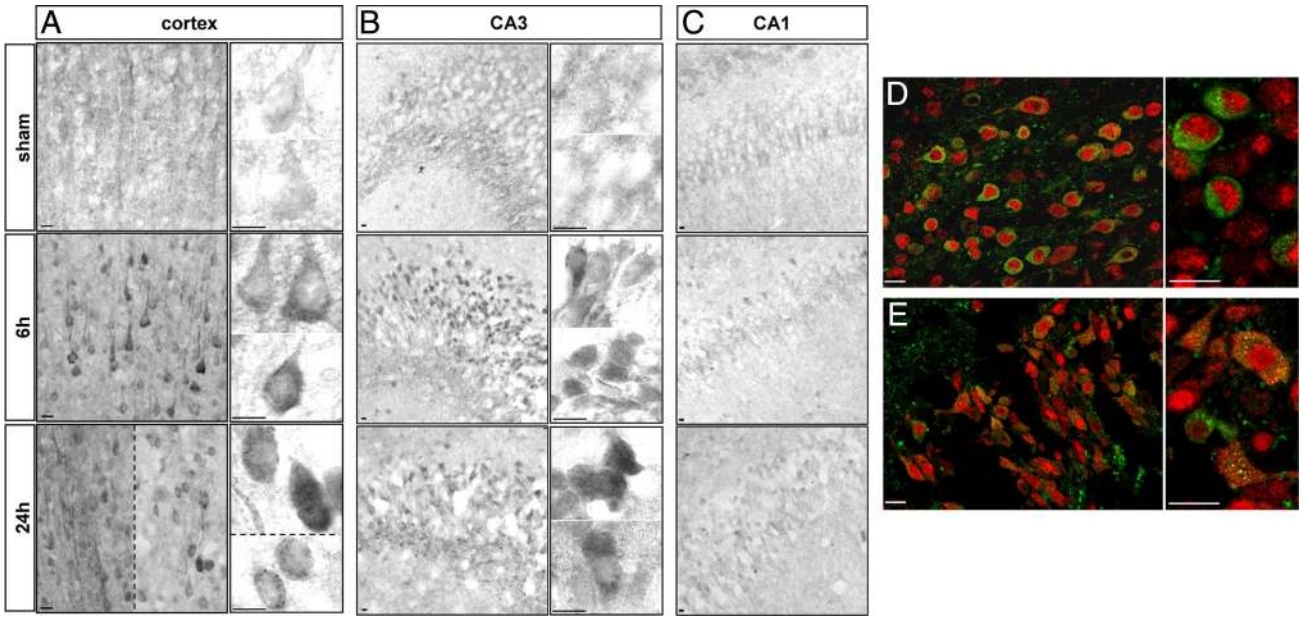

Figure 2. Effect of hypoxia-ischemia on LC3 distribution. **A** and **B:** Immunohistochemistry shows a strong increase in LC3 expression from 6 hours after the insult, and high-magnification views show numerous LC3-positive dots (vesicles corresponding to autophagosomes) at 24 hours in the cortex (**A**) mainly in the border of the lesion (**left side** of the dotted line) but also in some cells inside the lesion (**right side** of the dotted line and **lower side** in high magnification) and in the hippocampus essentially in CA3 (**B**). High magnifications of two or more representative neurons are shown for the cortex and CA3 illustrating the increase in the granular labeling of LC3 from 6 hours after hypoxia-ischemia. **C:** No change is detectable in CA1. **D** and **E:** Increase in punctate LC3 occurs in neurons as shown by confocal microscopy of double immunolabeling at 24 hours for NeuN (red) and LC3 (green) in cortex (**D**) and CA3 (hippocampus, **E**). Scale bars: 10 μm.

and hippocampus (Figure 5D): AP activity was raised significantly above the level of a sham animal in hippocampal extracts at 6 and 24 hours (161 ± 16% at 6 hours, 155 ± 9% at 24 hours) and in cortical extracts at 24 hours (137 ± 10%).

As illustrated for 24 hours after the insult in Figure 5E, AcHex histochemistry revealed an increase in the number and size of positive dots in some cortical and CA3 cells from 6 hours. In sections Nissl-stained after the histochemical procedure, the cells with strong AcHex

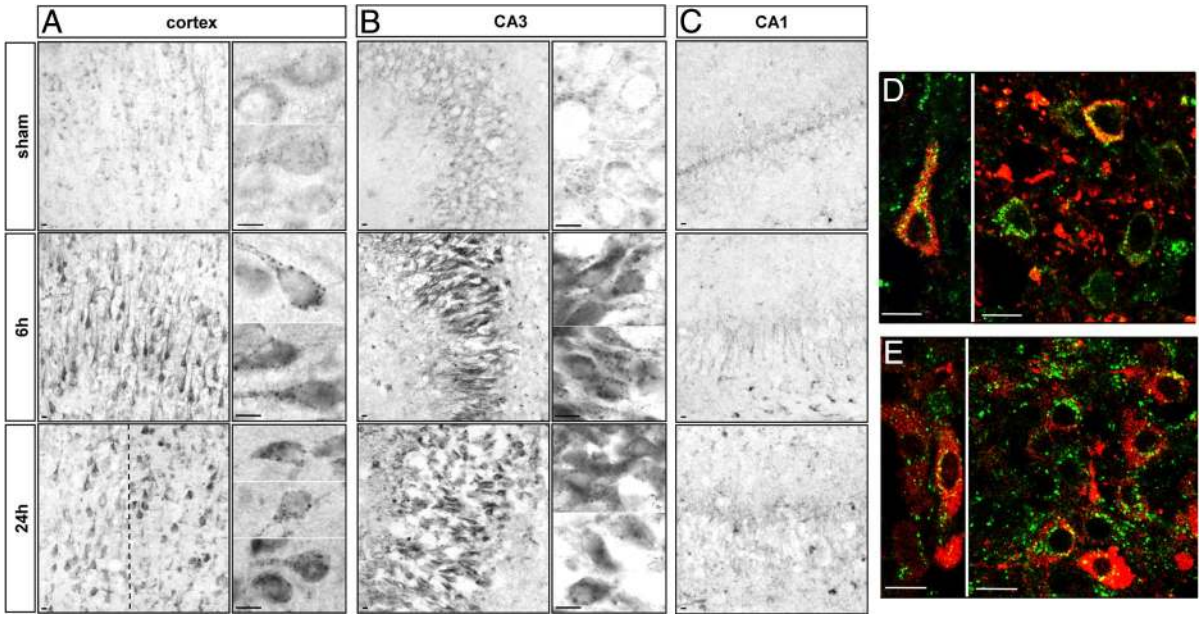

Figure 3. Effect of hypoxia-ischemia on LAMP1 expression and distribution. **A–C:** Immunohistochemistry after hypoxia-ischemia shows an increase in the LAMP1-positive dots at 6 and 24 hours in the cortex (**A**) in the border of the lesion (**left side** of the dotted line) but also in some cells inside the lesion (**right side** of the dotted line) and CA3 (**B**). High magnifications of two or more representative neurons are shown for the cortex and CA3, illustrating the substantial increase in the size of LAMP1-positive vesicles from 6 hours after hypoxia-ischemia. **C:** No change is detectable in CA1. **D** and **E:** Confocal microscopy reveals that the increase in LAMP1 occurs in neurons as shown by double immunolabeling for microtubule-associated protein 2 (red) and LAMP1 (green) at 24 hours in cortex (**D**) and CA3 (**E**). Scale bars: 10 μm.

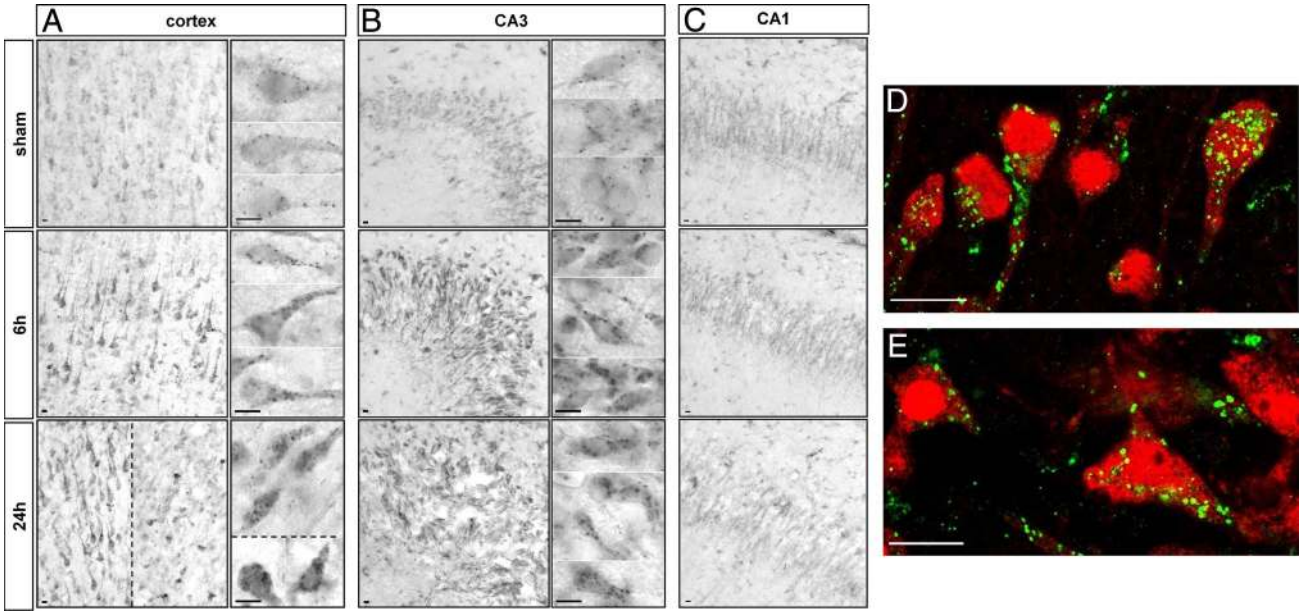

Figure 4. Effect of hypoxia-ischemia on cathepsin D expression and distribution. **A–C:** Immunohistochemistry after hypoxia-ischemia shows an increase in the cathepsin D-positive dots at 6 and 24 hours in the cortex (**A**) in the border of the lesion (**left side** of the dotted line) but also in some cells inside the lesion (**right side** of the dotted line and **lower side** in high magnification) and CA3 (**B**). High magnifications of two or more representative neurons are shown for the cortex and CA3, illustrating the substantial increase in the size of cathepsin D-positive vesicles from 6 hours after hypoxia-ischemia. **C:** No change is detectable in CA1. **D** and **E:** Confocal microscopy reveals that the cathepsin D increase occurs in neurons, as shown by double immunolabeling at 24 hours for NeuN (red) and cathepsin D (green) in cortex (**D**) and CA3 (**E**). Scale bars: 10 μm.

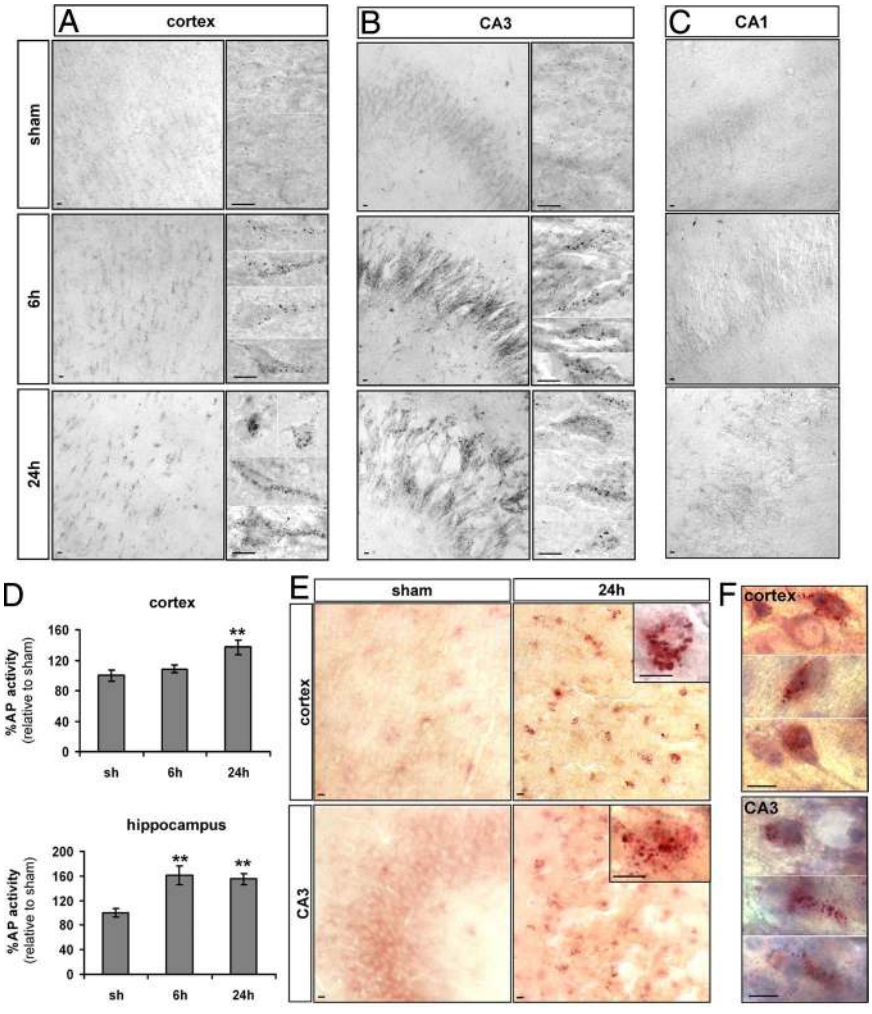

Figure 5. Effect of hypoxia-ischemia on lysosomal enzyme activities. **A–C:** Histochemistry for AP shows a strong increase in its activity (black dots) 6 and 24 hours after HI in the cortex (**A**) and CA3 (**B**). High magnifications of two or more representative neurons are shown for the cortex and the CA3, illustrating the strong increase of AP activity from 6 hours after hypoxia-ischemia. **C:** No change in AP activity is detectable in CA1. **D:** Enzyme assays confirm the increase in AP activity at 24 hours in the cortex and from 6 hours in the hippocampus. Data represents mean ± SEM. Comparisons with sham by *t*-test: $^{**}P < 0.01$; $n = 7$. **E:** Histochemistry for AcHex shows a strong increase in its activity in the cortex and CA3 after hypoxia-ischemia and (**F**) the combination with a cresyl violet stain shows that the cells with increased AcHex activity at 24 hours are neurons with nonpyknotic nuclei as illustrated by three representative neurons. Scale bars: 10 μm.

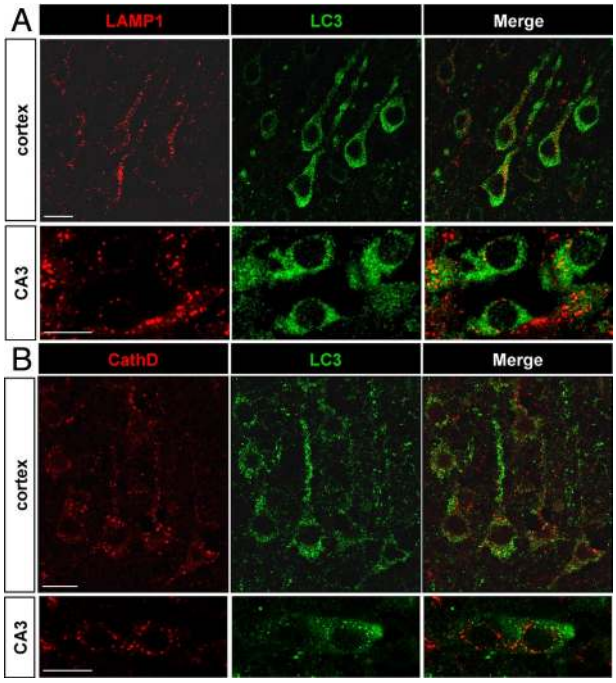

Figure 6. Relationship between autophagosomes and lysosomes. **A** and **B:** The increase in punctate LC3 labeling (green) and in lysosomal markers (red) occurs in the same neurons, as is here demonstrated at 6 hours for LAMP1 (**A**) and at 24 hours for cathepsin D (**B**) in the cortex and CA3 with confocal microscopy. Scale bars: 10 μm.

activity could be seen to display a neuronal morphology (Figure 5F).

To evaluate whether the increases in autophagosomes and lysosomal activities occurred in the same neurons, we performed double-immunolabeling experiments with the autophagosomal marker LC3 and the lysosomal markers cathepsin D and LAMP1 (Figure 6) at 6 and 24 hours. Most of the cells with strong punctate LC3 labeling displayed also an increase in LAMP1 or cathepsin D labeling, as shown in Figure 6, A and B, indicating that the increases in autophagosomes and lysosomes occurred in the same neurons.

Relationship between Autophagy and Neuronal Cell Death

To investigate the relationship between autophagy and other modes of cell death, the presence of apoptosis and necrosis after neonatal cerebral HI was analyzed by Western blot of cleaved caspase-3, as a marker of caspase-dependent apoptosis, and the 150-kDa calpain-dependent cleavage of the α-fodrin, as a marker of necrosis, as has been described in previous studies.[15,24,25]

In the Cortex

Western blot showed that 150-kDa α-fodrin product appeared very early after the insult, being strongly in-

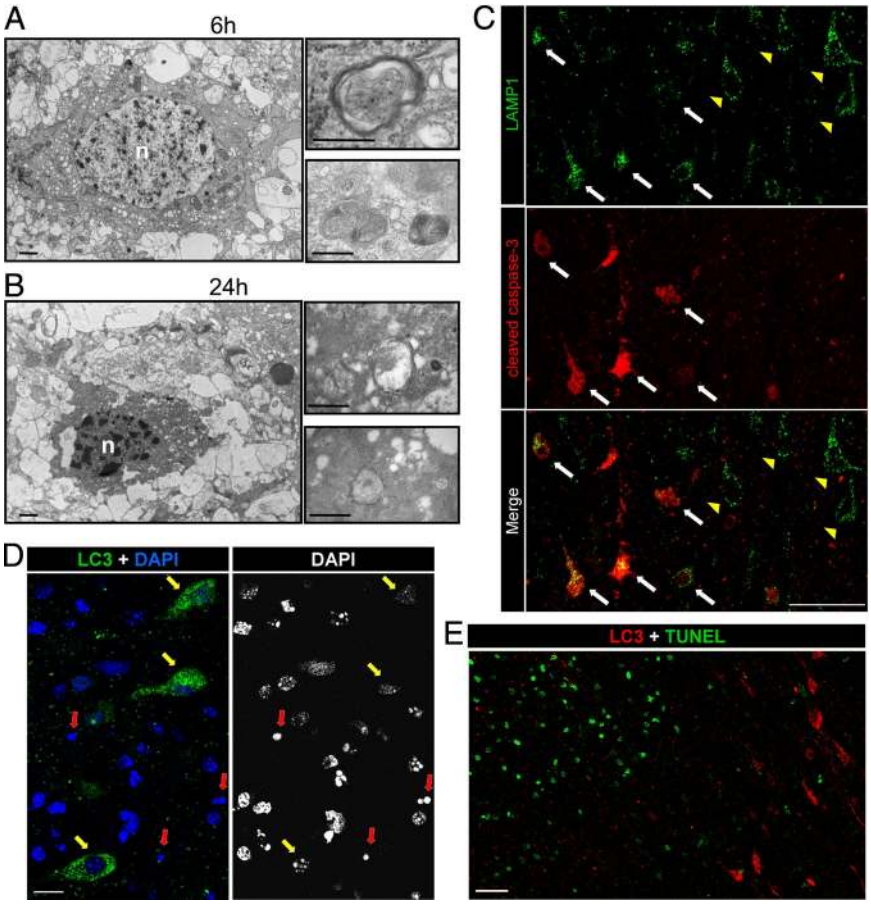

Figure 7. Relationship between autophagy and apoptosis in the cortex 24 hours after hypoxia-ischemia. **A** and **B:** Electron micrographs show neurons 6 hours (**A**) and 24 hours (**B**) after hypoxia-ischemia displaying numerous multimembrane vacuoles (putative autophagosomes) containing cytoplasmic material such as mitochondria, as illustrated at high magnification. Note the chromatin condensation in the nucleus (n) and the cytoplasmic shrinkage. Bars: 1 μm (**left panels**) and 0.5 μm (**right panels**). **C:** Double immunolabeling against LAMP1 (green) and cleaved caspase-3 (red) at 24 hours shows that the increase in LAMP1 is detectable in cortical neurons either positive (**white arrows**) or negative (**yellow arrowheads**) for cleaved caspase-3. Bars: 50 μm. **D:** Cortical neurons expressing strong punctate LC3 labeling at 24 hours after hypoxia-ischemia display little if any chromatin clumping (**yellow arrows**), and their nuclei are not pyknotic (**red arrows**) as demonstrated by co-labeling with 4′,6′-diamidino-2-phenylindole (DAPI) staining. Bars: 10 μm. **E:** These neurons were never TUNEL positive, as shown here for 24 hours. Scale bars: 50 μm.

creased by 30 minutes in comparison with a sham animal (30 minutes: 1220 ± 237%; 4 hours: 2488 ± 383%; 6 hours: 2708 ± 170%; 24 hours: 3068 ± 89%) (Supplemental Figure S1A, see *http://ajp.amjpathol.org*). Activation of caspase-3 appeared later, starting at 6 hours (758 ± 53%), becoming very strong at 24 hours (2864 ± 387%) (Supplemental Figure S1B, see *http://ajp.amjpathol.org*). The caspase-dependent α-fodrin band (120 kDa), which is a less sensitive marker of caspase activity than directly detected cleaved caspase-3, likewise appeared late, being detectable only at 24 hours (Supplemental Figure S1A, see *http://ajp.amjpathol.org*).

Electron microscopy revealed dying neurons displaying intense vacuolization and numerous autophagosomes in their cytosol. These were already detectable at 6 hours post-HI and were more abundant at 24 hours (Figure 7, A and B). High magnifications showed double-membrane structures encircling cytoplasmic regions including organelles. These dying neurons displayed also some criteria of apoptosis such as chromatin condensation, cytoplasmic shrinkage, and relatively good preservation of organelles such as mitochondria.

Then, we investigated the relationship between autophagy and apoptosis using several markers of the autophagic (LAMP1 and LC3) and the apoptotic (cleaved caspase-3 and TUNEL) pathways. First, double labeling for cleaved caspase-3 and LAMP1 revealed that some cortical neurons with strong LAMP1 staining were negative for cleaved caspase-3, whereas others, located closer to the center of the lesion, were positive for both (Figure 7C). Similar observations were obtained using double labeling for cathepsin D and cleaved caspase-3 (data not shown).

As demonstrated with 4′,6′-diamidino-2-phenylindole staining, the neurons expressing strong punctate LC3 labeling displayed nuclei with some degree of chromatin condensation but never a pyknotic nucleus (Figure 7D). Furthermore, double labeling between LC3 and TUNEL showed that LC3-positive neurons were never positive for TUNEL at 24 hours (Figure 7E), even in the center of the lesion (left in Figure 7E) where TUNEL-positive cells were numerous. The same was found at later times (48 and 72 hours; data not shown).

In the Hippocampus

As for the cortex, Western blot showed that 150-kDa α-fodrin product increased from 30 minutes (30 minutes: 505 ± 90%; 4 hours: 982 ± 146%; 6 hours: 1034 ± 176%; 24 hours: 1405 ± 128%) (Supplemental Figure S1C, see *http://ajp.amjpathol.org*). Activation of caspase-3 started weakly at 6 hours (273 ± 28%) and reached its maximal level at 24 hours (1263 ± 146%) (Supplemental Figure S1D, see *http://ajp.amjpathol.org*).

Interestingly the expression of apoptotic (cleaved caspase-3 and TUNEL) and autophagic markers (LAMP1, cathepsin D, and LC3) were regionally distinct (Figure 8). Caspase-3-positive neurons started to be detected in CA1, and the dentate gyrus at 6 hours were more numerous at 12 hours (data not shown) and extended throughout CA1 at 24 hours. Cleaved caspase-3 labeling was restricted to CA1 and the dentate gyrus (Figure 8B; Supplemental Figure S2D, see *http://ajp.amjpathol.org*), whereas LAMP1 staining was largely restricted to CA3, where it was detectable from 6 hours (Figures 8A and 3B). Similar results to those for LAMP1 were obtained for cathepsin D and LC3 (see Figures 2 and 4). In contrast, the spatial distribution of TUNEL staining resembled that for cleaved caspase-3, being mainly located in CA1 and the dentate gyrus, but it appeared later, at 24 hours (Figure 8D).

Immunohistochemistry against LC3 combined with a Nissl stain confirmed the much stronger LC3 staining in CA3 than CA1 and showed cell nuclei with multiple clumps of condensed chromatin in CA1 but only minor nuclear changes in CA3 (Figure 8C).

In view of these differences, we investigated the neuronal ultrastructure in CA1 and CA3 neurons. Twenty-four hours after HI, CA3 neurons displayed some striking features of autophagic cell death (Figure 8E), ie, numerous autophagosomes and autolysosome-like structures with normal or slightly condensed chromatin. At the same time point, CA1 neurons showed a different phenotype involving a combination of necrotic and apoptotic features: plasma membrane rupture, fragmented chromatin in the nuclei, and strongly swollen organelles (Figure 8F).

Discussion

The present study investigated the involvement of autophagy in a severe rat model of perinatal asphyxia. This model was originally developed in adult rats by Levine[21] and was adapted in the 1980s by Rice et al[19] for rat pups. The use of 7-day-old rat pups, as here, is standard for this model, because at this stage, the rat brain is developmentally similar to that of human newborns near term (34- to 35-week gestation).[26,27]

Neonatal HI Enhances Autophagic Flux in Cortical and CA3 Neurons

Excitotoxicity is one of the main pathophysiological mechanisms mediating neuronal death after cerebral HI, due in part to the excessive stimulation of *N*-methyl-D-aspartate receptors by excitatory amino acids such as glutamate.[28] Previous studies focusing on excitotoxicity-related neuronal death have suggested that autophagy could be implicated in mediating cell death in both *in vitro* and *in vivo* models of excitotoxicity. *N*-Methyl-D-aspartate-induced neuronal death in organotypic hippocampal slices has been shown to involve autophagy,[11] and in an *in vitro* model of amyotrophic lateral sclerosis, Matyja et al[12] demonstrated the involvement of autophagy in motor neuron degeneration induced by chronic glutamate excitotoxicity. The injection of kainate (a glutamate receptor agonist) in the hippocampus or striatum of adult mice induced delayed neuronal death and autophagy.[13,14] Recent studies demonstrated an increase in the number of autophagosomes in cerebral ischemia in different adult[15–17] and neonatal models.[15,18] In particular, the combination

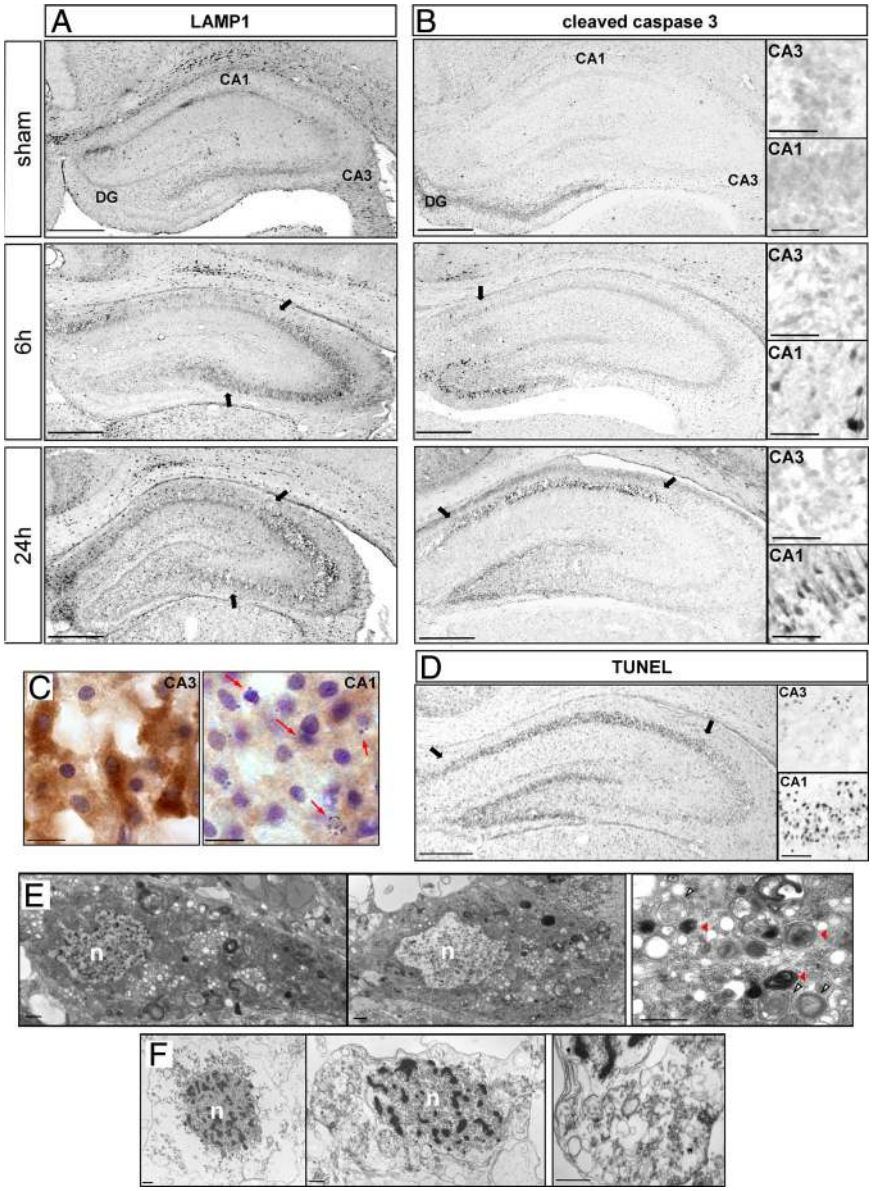

Figure 8. Relationship between autophagy and apoptosis in the hippocampus at 24 hours. **A** and **B:** Immunohistochemistry against LAMP1 (**A**) and cleaved caspase-3 (**B**) shows that the increases in LAMP1 expression and caspase-3 activation occur in different parts of the hippocampus. **A:** LAMP1 immunolabeling is strongly increased in CA3, whereas cleaved caspase-3 (**B**) is restricted to CA1 and dentate gyrus. High magnifications are representative of cleaved caspase-3-positive cells in CA1 (indicated by **arrows**) and in CA3. Scale bars: 0.5 mm and 50 μm in high magnification views. **C:** Immunohistochemistry against LC3 followed by a cresyl violet stain at 24 hours shows that CA3 neurons, strongly positive for LC3 staining, display nuclei with low chromatin fragmentation whereas highly condensed and pyknotic nuclei (**red arrows**) are detected in CA1 neurons, which display only faint LC3 staining. Bar: 10 μm. **D:** TUNEL staining at 24 hours is restricted to CA1 and dentate gyrus. High magnifications are representative of TUNEL-positive cells in CA1 (indicated by **arrows**) and in CA3. Bars: 0.5 mm and 50 μm in high magnifications. **E:** Electron micrographs of CA3 neurons at 24 hours show a very large number of autophagosomes in the cytosol. In a representative higher magnification figure (to the **right**), note the presence of double-membrane structures encircling organelles (**white arrowheads**) and the presence of autolysosomes (**red arrowheads**). The nucleus (n) of such CA3 neurons shows very little, if any, chromatin condensation. Bar: 1 μm. **F:** Electron micrographs of CA1 neurons at 24 hours after hypoxia-ischemia show a hybrid phenotype of cell death with a mixture of necrotic and apoptotic features, including plasma membrane rupture, chromatin condensation in the nucleus (n), and important swelling of organelles, as observed at high magnification. Scale bar: 1 μm.

of hypoxia and ischemia, which is necessary to produce brain damage in neonatal rats, was shown to induce autophagy in adults.[16] However it was not determined whether this increase in autophagy was due to an increase in autophagic flux or to a reduction in autophagosome elimination due to a defect in lysosomal fusion or degradation. In the present work, we have performed a detailed study of the whole process of autophagy after neonatal HI with the investigation of not only autophagosomal abundance but also lysosomal activity.

Autophagosome Increase

LC3-II is the only known Atg protein that remains in the membrane of the mature autophagosomes. LC3 immunolabeling and immunoblotting are therefore reliable methods to study autophagosome abundance.[29,30] Zhu et al[15] were the first to show by immunoblotting an increase in LC3-II in brain homogenates from the ipsilateral hemisphere in a mouse model of neonatal cerebral HI. More recently, Koike et al[18] demonstrated a significant increase in LC3-II specifically in the hippocampus in the same model. In the present study, we demonstrated that the LC3-II level was augmented in the four main cerebral regions affected by the HI: the cortex, hippocampus, striatum and thalamus. Autophagosome abundance was thus a common feature triggered by neonatal HI. These effects were purely ipsilateral to the carotid closure; the contralateral side also suffered hypoxia, but no increase in autophagy was detected in the contralateral cortex and hippocampus (Supplemental Figure S3, see *http://ajp.amjpathol.org*). Focusing on the ipsilateral cortex and hippocampus, we showed an increase in LC3 positive dots in some injured neurons from 6 hours and demonstrated in the hippocampus an enhancement of LC3 labeling specifically in CA3. This regional difference may be spe-

cies-specific since Koike et al[18] reported enhanced autophagy in CA1 pyramidal neurons in neonatal mice, and made no mention of such an effect in CA3. However, there were other differences between our model and theirs; notably, ours was more severe, with a longer period of hypoxia, which could affect the phenotype of the induced cell death.

Increase in Lysosomal Activity

Different studies demonstrated previously the involvement of lysosomal proteases in neuronal death, especially cathepsin B, after transient ischemia in the adult gerbil or monkey hippocampus[31,32] and after middle cerebral artery occlusion in adult rats.[17,33] We demonstrated here that the punctate expression of LAMP1, a major constituent of the lysosomal membrane,[34] was strongly increased in damaged neurons from 6 hours after HI, suggesting an increase in lysosomal activity. This was confirmed by study of the expression and/or activity of three different lysosomal enzymes: cathepsin D, AP, and AcHex, demonstrating an increased lysosomal activity following HI. The granular nature of the staining implies that the lysosomal enzymes were within intact lysosomes, which were not only more numerous but also larger (presumably autolysosomes), This indicates that the lysosomal enzymes did not leak out into the cytosol as had been suggested previously in a model of adult stroke.[35] We can conclude from this that the cell death was not due to the release from lysosomes of lytic enzymes.

By electron microscopy, we confirmed the increase in autolysosomes in dying neurons, indicating that fusion of autophagosomes with primary lysosomes occurred. Moreover, each lysosomal marker was increased in the same cerebral regions and in the same neurons as LC3. This demonstrated an enhancement of autophagic flux following neonatal HI.

The Relationship between Autophagy and Neuronal Death Depends on the Cerebral Region

The term "autophagic cell death" (type II) was introduced to describe a form of programed cell death morphologically distinct from apoptosis and characterized by the presence of intense autophagy.[6] The function of enhanced autophagy following cerebral ischemia has been investigated only in recent studies and a role in mediating neuronal death has been suggested. Thus, autophagic and lysosomal pathways have been shown to be activated by focal cerebral ischemia both in young rats[36] and in adults,[17] and in both cases intracerebroventricular administration of the autophagy inhibitor 3-methyladenine reduced the infarct volume. 3-Methyladenine also protected striatal neurons from kainate injection.[13] For neonatal HI, the role of enhanced autophagy remains unclear. Koike et al[18] demonstrated that specific inhibition of autophagy by the deletion of neuronal *Atg7* strongly protected the mouse hippocampus, but Carloni et al[37] proposed an opposite role of autophagy and showed that induction of autophagy with rapamycin decreased brain injury in rat neonatal HI. We analyzed, therefore, in our model of neonatal HI, the relationship between enhanced autophagy and neuronal death and observed important differences between the cortex and the hippocampus.

In the Cortex, Autophagy May Trigger an Apoptotic Pathway

Analysis of the ultrastructure of cortical cells showed the presence of dying neurons with numerous autophagosomes in their cytosol from 6 hours after HI, confirming enhanced autophagy following HI. However, these neurons never exhibited the morphology of pure autophagic cell death but also showed features of apoptosis, and cortical neurons with strong lysosomal expression (LAMP1 labeling) could also express cleaved caspase-3. These results indicate that simultaneous activation of autophagic and apoptotic mechanisms can occur in the same dying neuron. Rami et al[38] and Carloni et al[37] have also shown that an increase in Beclin 1 expression (the mammalian homologue of Atg6) colocalized with an activation of caspase-3 after adult cerebral ischemia or neonatal cerebral HI, respectively. Moreover, in our model, the neurons presenting strong autophagic features were mostly in the border of the lesion 24 hours after HI, were TUNEL-negative, displayed moderate chromatin condensation, and were never pyknotic, suggesting that autophagy could precede apoptosis. It remains to be determined if enhanced autophagy is present as a protective mechanism or if it contributes to neuronal death either as an independent mechanism or as a precursor of apoptosis. In fact, autophagic and apoptotic pathways share several points of interaction and their functional relationship is complex.[39] For example, full-length Atg5 is an inducer of autophagy, whereas an Atg5 fragment due to cleavage by calpain is proapoptotic.[40] The antiapoptotic protein Bcl-2 is also an antiautophagic protein through its interaction with Beclin 1.[41] Our results and the fact that inhibition of autophagy by 3-methyladenine treatment or *ATG7* deletion decreased caspase-3 activation in focal ischemia in young rats[36] and in neonatal HI[18,37] suggest that enhanced autophagy observed in the cortex may trigger apoptosis as described in some other cases of neuronal death.[42,43]

Involvement of Autophagy in "the Cell Death Continuum"

Our results indicate that cell death phenotypes after neonatal HI are very heterogeneous and cannot be categorized dichotomously as necrotic or apoptotic. Portera-Cailliau et al[4] were the first to report the existence of a "continuum" of apoptotic, necrotic, and overlapping morphologies after an excitotoxic injury in the neonatal forebrain (injection of acid kainic). Several subsequent studies have supported this view, describing the presence of "hybrid" cells with intermediate characteristics of

apoptosis and necrosis in various cerebral regions.[44,45] Moreover, markers of apoptosis (cleaved caspase-3) and necrosis (calpain-dependent fodrin breakdown product) can be expressed by the same damaged neurons.[46] Northington et al[5] proposed that the "continuum" could be explained by a failure to complete apoptosis in some dying cells due to a lack of energy and mitochondrial dysfunction. In fact, neonatal HI is known to induce a biphasic energy failure, the first occurring just after HI, followed by a recovery phase, and the second started about 24 hours after HI depending on the species.[47,48] Thus, the energy availability after HI is an important factor determining the phenotype of the cell death. Since autophagy is an energy-dependent mechanism, like apoptosis, but also a source of energy, and in the light of our results and others already cited, this "continuum" is still more complex since autophagy has to be included. On the one hand, autophagy may oppose apoptosis. By engulfing mitochondria, it may block the mitochondrial pathway of apoptosis and compromise the production of energy.[49] On the other hand, autophagy could allow apoptosis and delay necrotic cell death by providing energy substrates to the cell or through molecular interconnections with apoptosis. But sustained high level of autophagy could also lead by itself to the cell death by destruction of vital cellular components. Finally, all of the three cell death morphologies could occur in the cortex following neonatal HI giving mixed features of cell death.

In the Hippocampus, the Autophagic Phenotype of Cell Death Occurs Specifically in CA3

Previous studies, which performed cell counting in the different hippocampal regions, showed that CA1 displayed more apoptotic cells than CA3 following rat neonatal HI.[44,50] Moreover pharmacological caspase inhibition has been shown to prevent the decrease in CA1 neuronal density after rat neonatal HI.[51–53] In our model, caspase-3 activation was detected essentially in CA1, whereas enhanced autophagic flux occurred mainly in CA3. Unlike in the cortex, mixed features of autophagy and apoptosis were rare. The ultrastructure of the dying hippocampal cells showed that CA3 neurons displayed more classical autophagic features than in the cortex. Their nuclei presented only moderately condensed chromatin, and their cytosol contained several autophagosomes. CA1 neuronal cell death morphology corresponded more to the "continuum" described by Portera-Cailliau et al[4] and Sheldon et al[45] with features of both apoptosis (condensed chromatin) and necrosis (swelling or rupture of the cell membrane, vacuolization of the cytosol . . .).

These results suggest important differences in the neuronal responses to HI between CA3 and CA1. The reasons for this remain to be determined, but CA1 and CA3 are known to differ in their reaction to ischemic stimuli. Regions in the Ammon's horn (CA1–CA4) can be distinguished according to their morphologies, their connectivity, and their electrophysiological properties reflecting basic molecular differences as has been demonstrated by proteomic or genomic analysis in adult rat hippocampus.[54–57] Differential susceptibility to insults, such as seizures or HI, between CA1 and CA3 might result from their distinct patterns of protein/gene expression, and globally, CA1 appeared to present a basal molecular profile that makes it more vulnerable to apoptosis, at least in adult rats,[54,57] but less is known about the neonatal hippocampus.

It was shown in hippocampal slice cultures that oxygen-glucose deprivation had opposite effects on *N*-methyl-D-aspartate currents between CA1 and CA3 neurons. An intracellular increase in calcium enhanced *N*-methyl-D-aspartate responses in the vulnerable CA1 neurons, but transiently depressed them in the more resistant CA3 neurons.[58] This was partially explained by the fact that energy deprivation differentially changed the kinase/phosphatase balance, increasing tyrosine kinase activity in CA1 and phosphatase activity in CA3.[59] It has been also shown that acidosis during oxygen-glucose deprivation had a strong protective effect on CA3 neurons but virtually none on CA1.[60] Moreover, Mattiasson et al[61] showed that the formation of reactive oxygen species and mitochondrial permeability transition pore activation induced by calcium were higher in mitochondria isolated from the CA1 than from the CA3. These differences have been invoked to explain why CA1 is much more vulnerable in neonatal HI.[44,45] Our results suggest an additional explanation. The enhanced autophagic flux in CA3 could be initially protective, because it could counteract energy depletion and prevent necrosis or eliminate deficient mitochondria and reduce apoptosis. But persistent enhanced autophagy would finally lead to late neuronal death given that CA3 showed also a progressive loss of neurons from 6 hours to 1 week (Supplemental Figure S2, A–C, see *http://ajp.amjpathol.org*). Furthermore, we were not able to detect any increase in cleaved caspase-3 in CA3 at any stage (Supplemental Figure S2D, see *http://ajp.amjpathol.org*).

In conclusion, we here report that severe rat neonatal HI induced a strong increase in autophagic flux in some damaged neurons. Even though we could not define the exact role of this enhanced autophagy, our results suggest a role in mediating delayed neuronal death that varies according to the cerebral area. In the cortex, autophagy seems to be closely linked to apoptosis and may trigger it. By contrast, in the hippocampus, enhanced autophagy affected CA3 neurons rather specifically and seems to be independent of apoptosis. We very recently showed that inhibition of autophagy with 3-methyladenine was protective in a model of focal cerebral ischemia in young rats.[36] The present results may have clinical implications, because autophagy could be a promising therapeutic target, but its regional specificity will need to be taken into account.

Acknowledgments

We thank Guylène Magnin, Florine Fonknechten, Coralie Rummel and Vincent Mottier for technical assistance, Jean-Yves Chatton and Yannick Krempp of the Cellular Imaging Facility (University of Lausanne) for experimental

support, and the Centre of Electron Microscopy of the University of Lausanne for the use of their electron microscopes.

References

1. Volpe JJ: Perinatal brain injury: from pathogenesis to neuroprotection. Ment Retard Dev Disabil Res Rev 2001, 7:56–64
2. Ferriero DM: Neonatal brain injury. N Engl J Med 2004, 351:1985–1995
3. Sahni R, Sanocka UM: Hypothermia for hypoxic-ischemic encephalopathy. Clin Perinatol 2008, 35:717–734
4. Portera-Cailliau C, Price DL, Martin LJ: Excitotoxic neuronal death in the immature brain is an apoptosis-necrosis morphological continuum. J Comp Neurol 1997, 378:70–87
5. Northington FJ, Zelaya ME, O'Riordan DP, Blomgren K, Flock DL, Hagberg H, Ferriero DM, Martin LJ: Failure to complete apoptosis following neonatal hypoxia-ischemia manifests as "continuum" phenotype of cell death and occurs with multiple manifestations of mitochondrial dysfunction in rodent forebrain. Neuroscience 2007, 149:822–833
6. Clarke PGH: Developmental cell death: morphological diversity and multiple mechanisms. Anat Embryol 1990, 181:195–213
7. Clarke PGH, Puyal J, Vaslin A, Ginet V, Truttmann A: Multiple types of programmed cell death and their relevance to perinatal brain damage. In perinatal brain damage: from pathogenesis to neuroprotection, chp 3. Edited by LA Ramenghi, P Evrard, and E. Mercuri. Mariani Foundation Paediatric Neurology Series 19, John Libbey Eurotext, Montrouge, France, 2008, pp. 23–35
8. Shintani T, Klionsky DJ: Autophagy in health and disease: a double-edged sword. Science 2004, 306:990–995
9. Codogno P, Meijer AJ: Autophagy and signaling: their role in cell survival and cell death. Cell Death Differ 2005, 12:1509–1518
10. Boland B, Nixon RA: Neuronal macroautophagy: from development to degeneration. Mol Aspects Med 2006, 27:503–519
11. Borsello T, Croquelois K, Hornung JP, Clarke PGH: *N*-Methyl-D-aspartate-triggered neuronal death in organotypic hippocampal cultures is endocytic, autophagic and mediated by the c-Jun N-terminal kinase pathway. Eur J Neurosci 2003, 18:473–485
12. Matyja E, Taraszewska A, Nagańska E, Rafałowska J: Autophagic degeneration of motor neurons in a model of slow glutamate excitotoxicity in vitro. Ultrastruct Pathol 2005, 29:331–339
13. Shacka JJ, Lu J, Xie ZL, Uchiyama Y, Roth KA, Zhang J: Kainic acid induces early and transient autophagic stress in mouse hippocampus. Neurosci Lett 2007, 414:57–60
14. Wang Y, Han R, Liang ZQ, Wu JC, Zhang XD, Gu ZL, Qin ZH: An autophagic mechanism is involved in apoptotic death of rat striatal neurons induced by the non-*N*-methyl-D-aspartate receptor agonist kainic acid. Autophagy 2008, 4:214–226
15. Zhu C, Wang X, Xu F, Bahr BA, Shibata M, Uchiyama Y, Hagberg H, Blomgren K: The influence of age on apoptotic and other mechanisms of cell death after cerebral hypoxia-ischemia. Cell Death and Diff 2005, 12:162–176
16. Adhami F, Liao G, Morozov YM, Schloemer A, Schmithorst VJ, Lorenz JN, Dunn RS, Vorhees CV, Wills-Karp M, Degen JL, Davis RJ, Mizushima N, Rakic P, Dardzinski BJ, Holland SK, Sharp FR, Kuan CY: Cerebral ischemia-hypoxia induces intravascular coagulation and autophagy. Am J Pathol 2006, 169:566–583
17. Wen YD, Sheng R, Zhang LS, Han R, Zhang X, Zhang XD, Han F, Fukunaga K, Qin ZH: Neuronal injury in rat model of permanent focal cerebral ischemia is associated with activation of autophagic and lysosomal pathways. Autophagy 2008, 4:762–769
18. Koike M, Shibata M, Tadakoshi M, Gotoh K, Komatsu M, Waguri S, Kawahara N, Kuida K, Nagata S, Kominami E, Tanaka K, Uchiyama Y: Inhibition of autophagy prevents hippocampal pyramidal neuron death after hypoxic-ischemic injury. Am J Pathol 2008, 172:454–469
19. Rice JE, Vannucci RC, Brierley JB: The influence of immaturity on hypoxic-ischemic brain damage in the rat. Ann Neurol 1981, 9:131–141
20. Boland B, Kumar A, Lee S, Platt FM, Wegiel J, Yu WH, Nixon RA: Autophagy induction and autophagosome clearance in neurons: relationship to autophagic pathology in Alzheimer's disease. J Neurosci 2008, 28:6926–6937
21. Levine S: Anoxic-ischemic encephalopathy in rats. Am J Pathol 1960, 36:1–17
22. Gömöri G: Distribution of acid phosphatase in tissues under normal and under pathologic conditions. Arch Path 1941, 32:189–199
23. Katayama Y, Kobatake H, Shida H: A modified technique of histochemical demonstration for *N*-acetyl-β-hexosaminidase. Acta Histochem Cytochem 1976, 9:111–124
24. Wang KK: Calpain and caspase: can you tell the difference? Trends Neurosci 2000, 23:20–26
25. Ginet V, Puyal J, Magnin G, Clarke PG, Truttmann AC: Limited role of the c-Jun N-terminal kinase pathway in a neonatal rat model of cerebral hypoxia-ischemia. J Neurochem 2009, 108:552–562
26. Vannucci RC, Vannucci SJ: A model of perinatal hypoxic-ischemic brain damage. Ann NY Acad Sci 1997, 835:234–249
27. Hagberg H, Ichord R, Palmer C, Yager JY, Vannucci SJ: Animal models of developmental brain injury: relevance to human disease—a summary of the panel discussion from the Third Hershey Conference on Developmental Cerebral Blood Flow and Metabolism. Dev Neurosci 2002, 24:364–366
28. Johnston MV, Trescher WH, Ishida A, Nakajima W: Neurobiology of hypoxic-ischemic injury in the developing brain. Pediatr Res 2003, 49:735–741
29. Kabeya Y, Mizushima N, Ueno T, Yamamoto A, Kirisako T: Noda T. Kominami E, Ohsumi Y, Yoshimori T: lC3, a mammalian homologue of yeast Apg8p, is localized in autophagosomes membranes after processing EMBO J 2000, 19:5720–5728
30. Tanida I, Ueno T, Kominami E: LC3 conjugation system in mammalian autophagy. Int J Biochem Cell Biol 2004, 36:2503–2518
31. Nitatori T, Sato N, Kominami E, Uchiyama Y: Participation of cathepsins B, H, and L in perikaryal condensation of CA1 pyramidal neurons undergoing apoptosis after brief ischemia. Adv Exp Med Biol 1996, 389:177–185
32. Kohda Y, Yamashima T, Sakuda K, Yamashita J, Ueno T, Kominami E, Yoshioka T: Dynamic changes of cathepsins B and L expression in the monkey hippocampus after transient ischemia. Biochem Biophys Res Commun 1996, 228:616–622
33. Seyfried D, Han Y, Zheng Z, Day N, Moin K, Rempel S, Sloane B, Chopp M: Cathepsin B and middle cerebral artery occlusion in the rat. J Neurosurg 1997, 87:716–723
34. Chen JW, Murphy TL, Willingham MC, Pastan I, August JT: Identification of two lysosomal membrane glycoproteins. J Cell Biol 1985, 101:85–95
35. Yamashima T, Tonchev AB, Tsukada T, Saido TC, Imajoh-Ohmi S, Momoi T, Kominami E: Sustained calpain activation associated with lysosomal rupture executes necrosis of the postischemic CA1 neurons in primates. Hippocampus 2003, 13:791–800
36. Puyal J, Vaslin A, Mottier V, Clarke PGH: Postischemic treatment of neonatal cerebral ischemia should target autophagy. Ann Neurol 2009, doi: 10.1002/ana.21714
37. Carloni S, Buonocore G, Balduini W: Protective role of autophagy in neonatal hypoxia-ischemia induced brain injury. Neurobiol Dis 2008, 32:329–339
38. Rami A, Langhagen A, Steiger S: Focal cerebral ischemia induces up-regulation of Beclin 1 and autophagy-like cell death. Neurobiol Dis 2008, 29:132–141
39. Maiuri MC, Zalckvar E, Kimchi A, Kroemer G: Self-eating and self-killing: crosstalk between autophagy and apoptosis. Nat Rev Mol Cell Biol 2007, 8:741–752
40. Yousefi S, Perozzo R, Schmid I, Ziemiecki A, Schaffner T, Scapozza L, Brunner T, Simon HU: Calpain-mediated cleavage of Atg5 switches autophagy to apoptosis. Nat Cell Biol 2006, 8:1124–1132
41. Pattingre S, Tassa A, Qu X, Garuti R, Liang XH, Mizushima N, Packer M, Schneider MD, Levine B: Bcl-2 antiapoptotic proteins inhibit Beclin 1-dependent autophagy. Cell 2005, 122:927–939
42. Xue L, Fletcher GC, Tolkovsky AM: Autophagy is activated by apoptotic signalling in sympathetic neurons: an alternative mechanism of death execution. Mol Cell Neurosci 1999, 14:180–198
43. Canu N, Tufi R, Serafino AL, Amadoro G, Ciotti MT, Calissano P: Role of the autophagic-lysosomal system on low potassium-induced apoptosis in cultured cerebellar granule cells. J Neurochem 2005, 92:1228–1242
44. Nakajima W, Ishida A, Lange MS, Gabrielson KL, Wilson MA, Martin LJ, Blue ME, Johnston MV: Apoptosis has a prolonged role in the neurodegeneration after hypoxic ischemia in the newborn rat. J Neurosci 2000, 20:7994–8004
45. Sheldon RA, Hall JJ, Noble LJ, Ferriero DM: Delayed cell death in

neonatal mouse hippocampus from hypoxia-ischemia is neither apoptotic nor necrotic. Neurosci Lett 2001, 304:165–168
46. Blomgren K, Zhu C, Wang X, Karlsson JO, Leverin AL, Bahr BA, Mallard C, Hagberg H: Synergistic activation of caspase-3 by m-calpain after neonatal hypoxia-ischemia: a mechanism of "pathological apoptosis?" J Biol Chem 2001, 276:10191–10198
47. Vannucci RC, Towfighi J, Vannucci SJ: Secondary energy failure after cerebral hypoxia-ischemia in the immature rat. J Cereb Blood Flow Metab 2004, 24:1090–1097
48. Lorek A, Takei Y, Cady EB, Wyatt JS, Penrice J, Edwards AD, Peebles D, Wylezinska M, Owen-Reece H, Kirkbride V, Cooper CE, Aldridge RF, Roth SC, Brown G, Delpy DT, Reynolds EOR: Delayed ("secondary") cerebral energy failure after acute hypoxia-ischemia in the newborn piglet: continuous 48-hour studies by phosphorus magnetic resonance spectroscopy. Pediatr Res 1994, 36:699–706
49. Tolkovsky AM, Xue L, Fletcher GC, Borutaite V: Mitochondrial disappearance from cells: a clue to the role of autophagy in programmed cell death and disease? Biochimie 2002, 84:233–240
50. Kawamura M, Nakajima W, Ishida A, Ohmura A, Miura S, Takada G: Calpain inhibitor MDL 28170 protects hypoxic-ischemic brain injury in neonatal rats by inhibition of both apoptosis and necrosis. Brain Res 2005, 1037:59–69
51. Cheng Y, Deshmukh M, D'Costa A, Demaro JA, Gidday JM, Shah A, Sun Y, Jacquin MF, Johnson EM, Holtzman DM: Caspase inhibitor affords neuroprotection with delayed administration in a rat model of neonatal hypoxic-ischemic brain injury. J Clin Invest 1998, 101:1992–1999
52. Adachi M, Sohma O, Tsuneishi S, Takada S, Nakamura H: Combination effect of systemic hypothermia and caspase inhibitor administration against hypoxic-ischemic brain damage in neonatal rats. Pediatr Res 2001, 50:590–595
53. Han BH, Xu D, Choi J, Han Y, Xanthoudakis S, Roy S, Tam J, Vaillancourt J, Colucci J, Siman R, Giroux A, Robertson GS, Zamboni R, Nicholson DW, Holtzman DM: Selective, reversible caspase-3 inhibitor is neuroprotective and reveals distinct pathways of cell death after neonatal hypoxic-ischemic brain injury. J Biol Chem 2002, 277:30128–30136
54. Gozal E, Gozal D, Pierce WM, Thongboonkerd V, Scherzer JA, Sachleben LR Jr, Brittian KR, Guo SZ, Cai J, Klein JB: Proteomic analysis of CA1 and CA3 regions of rat hippocampus and differential susceptibility to intermittent hypoxia. J Neurochem 2002, 83:331–345
55. Lein ES, Zhao X, Gage FH: Defining a molecular atlas of the hippocampus using DNA microarrays and high-throughput *in situ* hybridization. J Neurosci 24:3879–3889
56. Greene JG, Borges K, Dingledine R: Quantitative transcriptional neuroanatomy of the rat hippocampus: evidence for wide-ranging, pathway-specific heterogeneity among three principal cell layers. Hippocampus 2009, 19:253–264
57. Jackson TC, Rani A, Kumar A, Foster TC: Regional hippocampal differences in AKT survival signaling across the lifespan: implications for CA1 vulnerability with aging. Cell Death Differ 2009, 16:439–448
58. Grishin AA, Gee CE, Gerber U, Benquet PJ: Differential calcium-dependent modulation of NMDA currents in CA1 and CA3 hippocampal pyramidal cells. Neurosci 2004, 24:350–355
59. Gee CE, Benquet P, Raineteau O, Rietschin L, Kirbach SW, Gerber U: NMDA receptors and the differential ischemic vulnerability of hippocampal neurons. Eur J Neurosci 2006, 23:2595–2603
60. Cronberg T, Jensen K, Rytter A, Wieloch T: Selective sparing of hippocampal CA3 cells following in vitro ischemia is due to selective inhibition by acidosis. Eur J Neurosci 2005, 22:310–316
61. Mattiasson G, Friberg H, Hansson M, Elmér E, Wieloch T: Flow cytometric analysis of mitochondria from CA1 and CA3 regions of rat hippocampus reveals differences in permeability transition pore activation. J Neurochem 2003, 87:532–544